JACS Au
AN OPEN ACCESS JOURNAL OF THE AMERICAN CHEMICAL SOCIETY

pubs.acs.org/jacsau
Article

Ru-Nitrosyl Complex Salts as Efficient Catalysts for the Reversible CO_2 Hydrogenation/FA Dehydrogenation in Ionic Liquids

Published as part of JACS Au special issue "Advances in Small Molecule Activation Towards Sustainable Chemical Transformations".

José Tiago M. Correia,[†] Valeria Nori,[†] Mike S. B. Jørgensen, Alexander T. Nikol, and Martin Nielsen*

Cite This: JACS Au 2025, 5, 2114–2122

Read Online

ACCESS | Metrics & More | Article Recommendations | Supporting Information

ABSTRACT: We demonstrate that bench-stable ruthenium-PNP nitrosyl complex salts with different counteranions (Cl^-, BF_4^-, BPh_4^-, PF_6^-, and OTs^-) and a ruthenium-POP nitrosyl complex are competent (pre)catalysts for the CO_2 hydrogenation to formic acid (FA) at low temperatures in ionic liquids. Only a minor effect of variation of the counteranion was observed, and weakly basic ionic liquids such as EMIM OAc, BMIM OAc, and EMIM HCO_2 were suitable for this transformation, affording conversions up to 94 mol % formic acid compared to the ionic liquid (FA/IL) and turnover numbers (TONs) up to 1305. Importantly, the same catalytic system was also efficient for the dehydrogenation of formic acid back to CO_2 and H_2, affording conversions up to >95% (949 TON) after 3 h at 95 °C. To investigate the application of such protocols for hydrogen storage and transportation purposes, hydrogenation/dehydrogenation cycles were performed, showing that this new catalytic system can promote up to 10 reversible CO_2 hydrogenation/FA dehydrogenation cycles before losing its activity.

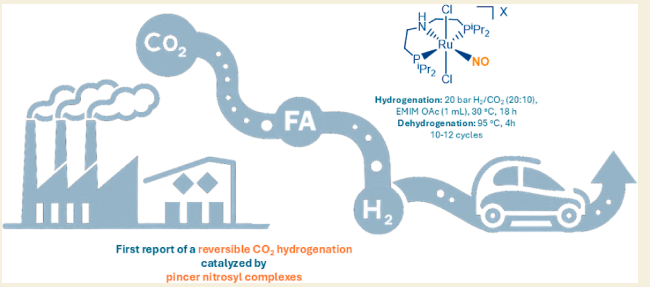

KEYWORDS: *ruthenium complexes, nitrosyl complexes, CO_2 valorization, dehydrogenation, hydrogen storage, bench-stable*

INTRODUCTION

Carbon capture and utilization (CCU) technologies consist of a set of strategies that allow for the capture and use of CO_2 from a gas stream feedstock for making industrially relevant products, such as commodity chemicals, fuels, and building materials. Such technologies aim at reducing the world's dependency on fossil resources and, at the same time, complement the large-scale efforts to prevent greenhouse gas emissions.[1−3] Despite its main role in the rapid and severe climate changes observed over the last century, CO_2 is an abundant, renewable, nontoxic, and economical carbon source.[1−5] It can be converted into a set of highly valuable chemicals, such as carbonates, carboxylic acids, amides, formic acid, and methanol.[4,5] Among them, formic acid (FA) stands out as a promising candidate for the long-term, safe, and practical storage of hydrogen (4.4 wt % H), connecting renewable energy and hydrogen fuel cells, and potentially closing an ideal carbon-free energy cycle.[6−12] The majority of already reported catalytic protocols for the reversible CO_2/FA interconversion rely on the use of additives and volatile solvents, or higher pressures of H_2/CO_2 (>40 bar), rendering these systems impractical for applications and scaling up for, for example, rechargeable hydrogen storage and release purposes. Other drawbacks are the harsh reaction conditions often used and the necessity of an inert atmosphere, due to the intrinsic nature of the catalysts employed (Chart 1a−e).[13−18] Aiming to overcome such limitations, our group recently developed a protocol employing a Ru-PNP pincer catalyst in ionic liquids (ILs) for the additive- and volatile solvent-free reversible CO_2/FA interconversion under very mild conditions showing high compatibility with continuous-flow conditions (Chart 1f).[19−21] Driven by the achievements in this first work, we embarked on a search for even more practical and applicable systems, which include screening for more reactive and stable (preferentially bench-stable) catalysts.

Widely known by their medicinal application as nitric oxide donors,[22−26] nitrosyl complexes have been found to be suitable for catalytic applications over the last two decades.[27−35] In catalysis, the nitrosyl ligand remains bonded to the metal center, acting as a stronger electron-withdrawing ancillary ligand than the carbonyl, or as a noninnocent ligand, changing the oxidation state of the metal center through its characteristic bent/linear interconversion.[22]

Received: January 15, 2025
Revised: April 7, 2025
Accepted: April 8, 2025
Published: April 15, 2025

Chart 1. Previously Reported Catalytic Systems for the CO_2/FA Interconversion That Do Not Require pH Adjustment or Any Other Additional Step (a–f)[a]

(a) 2014, Plietker et al.[4a]

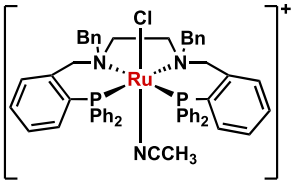

Hydrogenation: Dry ice/70 bar H_2, DBU/Toluene, 100 °C, 2 h
Dehydrogenation: 100 °C, 2 h
5 cycles

(b) 2014, Pidko et al[4b]

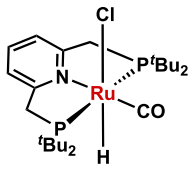

Hydrogenation: 40 bar H_2/CO_2 (1:1), DMF/DBU (30/5 mL), 65 °C, up to 3 h
Dehydrogenation: 90 °C, up to 1 h
5 cycles

(c) 2015, Czaun, Prakash, Olah et al[4c]

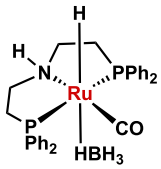

Hydrogenation: 75 bar H_2/CO_2 (3:1), Dioxane/H_2O (20/10 mL), NaOH (20 mmol), 70 °C, 5 h
Dehydrogenation: 70 °C, 5 h
5 cycles

(d) 2023, Igau, Fischmeister et al[4d]

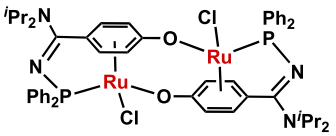

Hydrogenation: 60 bar H_2/CO_2 (1:1), DMSO (3 mL), 60 °C, 16-21 h
Dehydrogenation: 90 °C, up to 2.5 h
4 cycles

(e) 2023, Junge, Sponholz, Beller et al[4e]

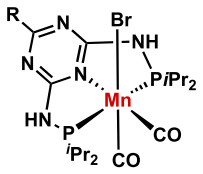

Dehydrogenation: FA/Lys (1:1), THF/H_2O (5/5 mL), 90 °C, 12 h
Capture: CO_2 (20 bar for 0.5 h or 2 bar for 6 h)
Hydrogenation: H_2 (80 bar), 85°C, 12 h
10 cycles

(f) 2023, Das, Nielsen et al[5]

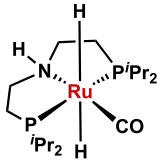

Hydrogenation: 20 bar H_2/CO_2 (20:10), EMIM OAc (2 mL), 25 °C, 18 h or 72 h
Dehydrogenation: 95 °C, 4 h
13 cycles

(g) This work

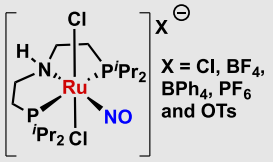

Hydrogenation: 20 bar H_2/CO_2 (20:10), EMIM OAc (1 mL), 30 °C, 18 h or 72 h
Dehydrogenation: 95 °C, 4 h
10-12 cycles

First report of a reversible CO_2 hydrogenation catalyzed by pincer nitrosyl complexes

[a]Our approach reporting for the first time a reversible CO2 hydrogenation catalyzed by pincer nitrosyl complexes (g).

Although the synthesis and characterization of a variety of nitrosyl complexes of base- and precious metals have appeared in the literature, most catalytic protocols described to date focus on the hydrogenation,[27−29] hydrosilylation,[34] or transfer hydrogenation[30,31] of carbonyls and alkenes, and on dehydrogenative couplings.[33] The only exception to this trend are the works from Plietker and co-workers, who employ the iron nitrosyl complex $[Bu_4N][Fe(CO)_3(NO)]$ and its derivative $[Bu_4N][Fe(CO)(PPh_3)_2(NO)]$ as efficient catalysts for a large number of organic transformations, such as allylic substitutions, Michael additions, C−H aminations, and cyclotrimerizations.[36−39] Narrowing down to pincer nitrosyl complexes exhibiting catalytic activity, there are very few examples reported in the literature, all of them in the aforementioned categories.[40−44]

Recently, in search for alternative catalysts to the well-established Ru-MACHO and its derivatives,[45−54] our group embarked on the synthesis and characterization of a set of bench-stable Ru-PNP-nitrosyl complex salts (PNP = $(^iPr_2PCH_2CH_2)_2NH$), and their application as (pre)catalysts in hydrogen-involving reactions.[55] The promising catalytic activity observed in our preliminary investigation prompted us to test such a family of catalysts in the CO_2 hydrogenation and FA dehydrogenation, adapting our recently described approach. Besides developing a more efficient and practical protocol, our investigation also aimed to study in which extension the nature of the (pre)catalyst counteranion affects the reaction outcome, which might be particularly relevant because the reaction medium is a salt as well. Herein, we present the first application of a nitrosyl complex for the mild, additive- and volatile-solvent-free, and reversible CO_2/FA interconversion (Chart 1g).

RESULTS AND DISCUSSION

CO_2 Hydrogenation

We started our investigation testing the activity of the PNP-Ru-NO salts **Ru-1** and **Ru-2**, using 1-ethyl-3-methylimidazolium acetate (EMIM OAc) as a solvent, due to its well-known capability of chemisorbing CO_2 (Table 1).[56] To our delight, both complexes (0.02 M in 1 mL of EMIM OAc, 0.25 mol % loading based on the amount of loaded CO_2) promoted the desired transformation, affording 85 and 87 mol %, respectively, of FA in IL (85% and 87% FA/IL) when subjected to 30 bars of CO_2/H_2 (10:20 bar) at 40 °C for 18 h (Table 1, entries 1−2). This corresponds to 68% and 70% yields, respectively, calculated from the amount of CO_2 available under the given conditions (see the Supporting Information for details). Lowering the temperature to 30 °C does not substantially affect the catalytic activity of the system (Table 1, entries 3−6) and we, therefore, decided to continue the screening at this temperature. Moreover, the system showed a high water tolerance. By adding 0.1 and 0.05 mL of water, the catalytic system retains its efficiency, resulting in 71% and 77% conversion of CO_2 into FA, respectively (Table 1, entries 4−5). We then tested PNP-Ru-NO salts **Ru-3**, **Ru-4**, and **Ru-5**, which all performed very similar to **Ru-2**, affording up to 94 mol % FA/IL (Table 1, entries 7−9). A POP-Ru-NO complex (**Ru-6**) showed much inferior reactivity (52 mol % FA/IL) under the same conditions employed to the PNP

https://doi.org/10.1021/jacsau.5c00051
JACS Au 2025, 5, 2114−2122

Table 1. Initial Temperature and Catalyst Screening for CO_2 Hydrogenation to FA[a]

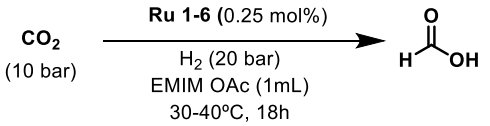

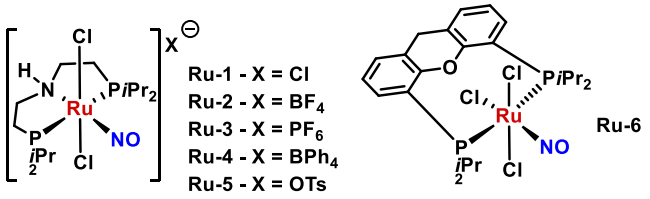

entry	catalyst [mol %][b]	T [°C]	FA/IL [mol %][c]	yield [%][b]	TON
1	**Ru-1**	40	85	68	270
2	**Ru-2**	40	87	70	280
3	**Ru-1**	30	78	62	250
4[d]	**Ru-1**	30	77	62	250
5[e]	**Ru-1**	30	71	56	220
6	**Ru-2**	30	88	70	280
7	**Ru-3**	30	93	74	300
8	**Ru-4**	30	87	70	280
9	**Ru-5**	30	94	75	300
10	**Ru-6**	30	52	42	170
11	**Ru-6**	40	70	56	220
12	$RuCl_3(NO)\cdot H_2O$[f]	30			

[a]Standard reaction conditions: **Ru-1**−**Ru-6** (0.02 mmol, 0.25 mol %), EMIM OAc (1 mL), 10:20 bar CO_2/H_2, 18 h. [b]Based on the amount of CO_2. [c]Determined by ^1H NMR. [d]0.05 mL of H_2O. [e]0.1 mL of H_2O. [f]0.5 mol %.

analogues (Table 1, entry 10). However, a significant increase in the formic acid formation (70 mol % FA/IL) was observed when the reaction temperature was increased to 40 °C (Table 1, entry 11). A control experiment using the precursor of all of the pincer Ru−NO complexes, $RuCl_3(NO)\cdot H_2O$, did not show any reactivity under the optimal conditions established at this stage of the study (Table 1, entry 12).

With these promising results in hand, we further investigated different parameters such as catalyst loading, overall pressure, CO_2/H_2 pressure ratio, and the nature of IL. The system was found to be highly responsive to the variation of the reaction parameters, as shown in Table 2. Decreasing the catalyst loading of **Ru-2** from 0.25 mol % (Table 2, entry 1) to 0.125 mol % and further to 0.05 mol % resulted in a significant decrease of conversion, affording merely 65 and 30 mol % FA/IL, respectively, after 18 h (Table 2, entries 2−3). As expected, the catalytic activity was restored by increasing the temperature from 30 to 60 °C, providing 82 mol % FA/IL with 0.05 mol % **Ru-2** (Table 2, entry 4). Keeping the catalyst loading at 0.25 mol %, a screening of ILs showed that BMIM OAc performs similarly to EMIM OAc (92 mol % FA/IL, entry 5, Table 2), while the ILs containing other counteranions, such as carbonate, formate, and diethylphosphate afforded lower conversions (Table 2, entries 6−8). These results indicate that the anion of the IL must be basic enough to promote the CO_2 chemisorption via NHC carbene formation and catalyst activation and/or to favor the equilibrium toward FA by its deprotonation upon formation. Decreasing the partial pressure of H_2 to 10 bar led to only 47 mol % FA/IL (38% NMR yield, Table 2, entry 9), showing that 20 bar of H_2 is necessary to afford FA in higher conversions when 10 bar of CO_2 is

Table 2. Screening of Catalyst Loading, CO_2/H_2 Pressure Ratio, Overall Pressure, and ILs for CO_2 Hydrogenation to FA[a]

entry	catalyst [mol %]	CO_2/H_2 [bar]/[bar]	IL	FA/IL [mol %][c]	yield [%][b]	TON
1	**Ru-2** [0.25]	10:20	EMIM OAc	88	63	250
2	**Ru-2** [0.125]	10:20	EMIM OAc	65	46	370
3	**Ru-2** [0.05]	10:20	EMIM OAc	30	24	480
4[d]	**Ru-2** [0.05]	10:20	EMIM OAc	82	66	1320
5	**Ru-2** [0.25]	10:20	BMIM OAc	92	74	300
6	**Ru-2** [0.25]	10:20	EMIM $MeCO_3$	74	59	240
7	**Ru-2** [0.25]	10:20	BMIM HCO_2	66	53	210
8	**Ru-2** [0.25]	10:20	EMIM $(EtO)_2PO_2$	38	30	120
9	**Ru-2** [0.25]	10:10	EMIM OAc	47	38	150
10	**Ru-2** [0.5]	5:10	EMIM OAc	57	>95	190

[a]Standard reaction conditions: **Ru-2** (0.004−0.04 mmol), IL (1 mL), CO_2/H_2, 18 h, 30 °C. [b]Based on the amount of CO_2. [c]Determined by ^1H NMR. [d]Reaction carried out at 60 °C.

employed. The catalytic activity of **Ru-2** in EMIM OAc was also tested under 5:10 bar of CO_2/H_2 (Table 2, entry 10). Under such conditions, 57 mol % FA/IL was obtained, which corresponds to >95% yield with respect to CO_2, highlighting that the system can be potentially productive in reactors with a lower pressure limit.

We also monitored the conversion over the time. The reaction reaches a plateau after 15 h at 30 °C, having already promoted the hydrogenation of CO_2 to FA in good conversion (up to 87% FA/IL, corresponding to 70% yield, Figure 1). After 48 h, FA is formed in practically 100% FA/IL (80% yield).

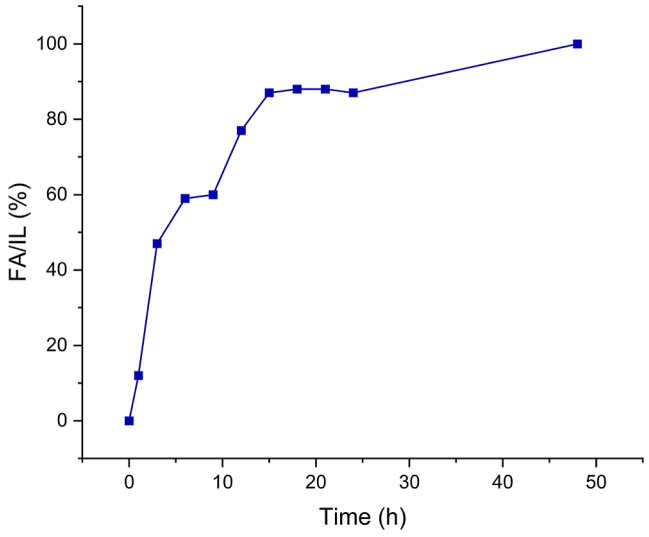

Figure 1. Conversion of CO_2 to FA vs time. Reaction conditions: **Ru-2** (0.004 mmol, 0.05 mol %), EMIM OAc (1 mL), CO_2/H_2 (10:20 bar), 30 °C.

https://doi.org/10.1021/jacsau.5c00051
JACS Au 2025, 5, 2114−2122

To gather more knowledge about the catalysts and our new catalytic system, we also tested a two-step approach where the CO_2 was captured by the IL, followed by a subsequent atmosphere exchange to H_2 for the catalytic hydrogenation process (Scheme 1). It is of paramount importance for the development of future CCU systems to demonstrate both steps of carbon capture and utilization in sequence one-pot under benign conditions, even as a proof of concept from a source of pure CO_2.

Scheme 1. CO_2 Capture and Subsequent Hydrogenation Experiment

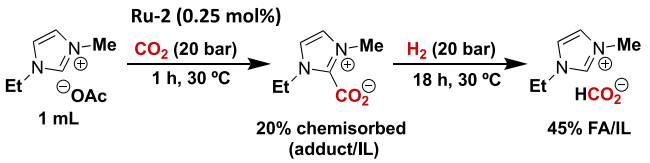

Initially, the system was charged with 20 bar CO_2 to EMIM OAc (1 mL) and **Ru-2** (0.02 M) for 1 h at 30 °C, which resulted in 20 mol % CO_2/IL as determined by the amount of chemisorbed CO_2 measured by NMR. The subsequent release of the CO_2 pressure and addition of 20 bar of H_2 afforded 45 mol % FA/IL after 18 h at 30 °C. As observed in our previous study,[19−21] the FA/IL ratio was higher than the chemisorbed CO_2/IL ratio. This discrepancy can be explained by an amount of physisorbed gaseous CO_2 in the IL, which stays in the IL during the gas change.

In a first approach to measure the reusability of the catalytic system and the maximum amount of FA it can sustain, the reaction mixture (**Ru-2** in 1 mL of EMIM OAc) was subjected to consecutive hydrogenation steps, in which the system was refilled with 30 bar (10:20 bar) of CO_2/H_2 mixture every 18 h (Figure 2). We observed a significant increment of the FA/IL ratio after the first refilling step (112%), and it reached a maximum of 117% at the third refiling step (fourth reaction) corresponding to a FA concentration of 7.6 M (or 6.9 mol kg^{-1} or 31.8 wt %), a highly competitive achievement compared to the recent literature.[19,57] The maximum amount was relatively constant over two more refilling steps, after which it started to decrease, indicating that dehydrogenation was taking place, even with the maintenance of the CO_2/H_2 atmosphere.

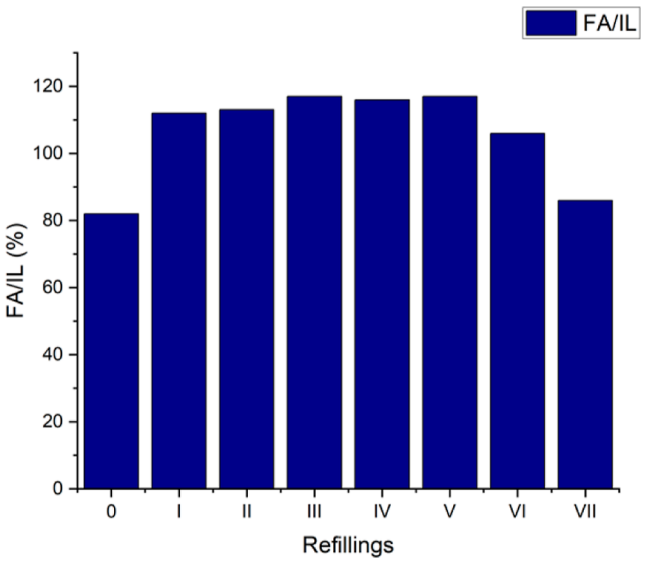

Figure 2. Refilling experiments showing the maximum amount of FA that can be formed after successive hydrogenation steps using the same reaction mixture. Reaction conditions: **Ru-2** (0.004 mmol, 0.05 mol %), EMIM OAc (1 mL), CO_2/H_2 (10:20 bar), 18 h, 30 °C.

Finally, in situ NMR and HR-MS investigations provided some insights into the fate of **Ru-1** (Figures S20, S21, S28, S29). The ^{31}P NMR suggested that single main new species is formed, and HR-MS identified a new complex resulting from substituting the two axial chlorido ligands essentially by deprotonated EMIM OAc, i.e., one *N*-heterocyclic carbene and one acetato is attached to an amido-based PNP-Ru-NO core. Whether the species identified in NMR is the same remains unclear, and it is likewise currently uncertain whether this complex is an inhibited off-cycle catalyst or a resting state of the active catalyst.

FA Dehydrogenation

Aiming at exploiting the system as a promising candidate for an energy storage technology based on CO_2−FA interconversion, we turned our investigation toward the FA dehydrogenation. Given their distinct pincer ligand frameworks, we started studying the reactivity of **Ru-2** and **Ru-6**, adapting the optimized reaction conditions for FA dehydrogenation previously reported by our group (i.e., EMIM OAc, 0.5 mol % catalyst, 80 °C). To our delight, both reactions showed very high conversions after 3 h (Table 3, entries 1 and 2). To identify the best reaction conditions, we screened different

Table 3. FA Dehydrogenation Optimization[a]

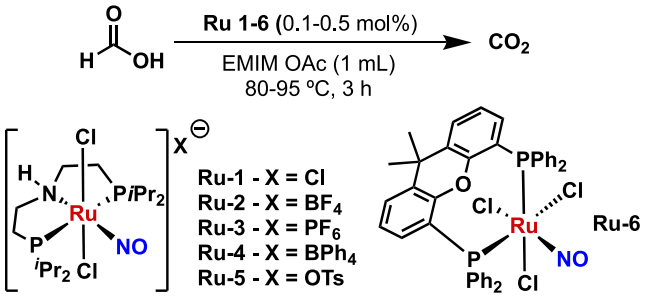

entry	catalyst [mol %]	T [°C]	IL	conv. [%][b]	TON
1	**Ru-2** [0.5]	80	EMIM OAc	93	202
2	**Ru-6** [0.5]	80	EMIM OAc	94	189
3	**Ru-2** [0.1]	80	EMIM OAc	67	683
4	**Ru-6** [0.1]	80	EMIM OAc	25	255
5	**Ru-2** [0.1]	95	EMIM OAc	94	958
6	**Ru-6** [0.1]	95	EMIM OAc	>95	>968
7	**Ru-1** [0.1]	95	EMIM OAc	>95	>968
8	**Ru-3** [0.1]	95	EMIM OAc	>95	>968
9	**Ru-4** [0.1]	95	EMIM OAc	90	917
10	**Ru-5** [0.1]	95	EMIM OAc	93	948
11	**Ru-1** [0.1]	95	BMIM OAc	>95	>968
12	**Ru-1** [0.1]	95	BMIM HCO_2	<5	
13	**Ru-1** [0.1]	95	EMIM $(EtO)_2PO_2$	<5	
14	$RuNOCl_3H_2O$ [1.0]	95	EMIM OAc	41	41

[a]Standard reaction conditions: **Ru-1**−**Ru-6** (0.013−0.066 mmol), EMIM OAc (1 mL), FA (0.5 mL, 13.25 mmol), 3 h under gentle flow of Ar. Gas composition is analyzed by GC-TCD. [b]Determined by ^1H NMR.

https://doi.org/10.1021/jacsau.5c00051
JACS Au 2025, 5, 2114−2122

parameters, such as catalyst loading, temperature, the other precatalysts (**Ru-1** and **Ru-3−5**), and different ILs (Table 3, entries 3−14). Lowering the catalyst loading from 0.5 to 0.1 mol % caused a decrease in conversion for both **Ru-2** and **Ru-6** (Table 3, entries 3 and 4).

Maintaining the catalyst loading at 0.1 mol % and increasing the temperature to 95 °C led to the recovery of the excellent conversions observed in the initial experiments (Table 3, entries 5 and 6). Under such conditions, **Ru-1** and **Ru-3−5** all afforded very high FA conversions within 3 h (Table 3, entries 7−10). The same behavior was observed when BMIM OAc was used instead of EMIM OAc (Table 3, entry 11), while no FA dehydrogenation was observed when using BMIM HCO_2 or EMIM $(EtO)_2PO_2$ (Table 3, entries 12 and 13). In a control experiment, the precursor of both PNP- and POP-Ru-NO complexes, $RuCl_3(NO)\cdot H_2O$, only afforded 41% conversion although the catalyst loading was 10 times higher than the optimized conditions (Table 3, entry 14).

To gather more information about the system under study, the progresses of the FA dehydrogenations employing **Ru-2** (PNP ligand) and **Ru-6** (POP ligand) were monitored at different time points over 3 h (Figure 3). The data show that

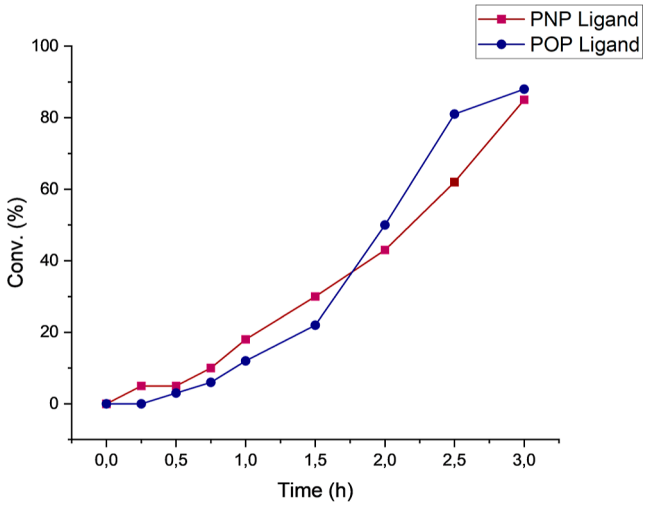

Figure 3. Dehydrogenation of FA vs time at 95 °C. Reactivity comparison between **Ru-2** and **Ru-6** 0.1 mol %.

the overall behavior of both catalysts is very similar over this period. Moreover, the catalyst/IL system appears pristine following complete FA conversion, demonstrating its unique potential in conducting hydrogenation/dehydrogenation cycles.

CO_2 Hydrogenation/FA Dehydrogenation Cycles

With the optimal conditions of both hydrogenation and dehydrogenation protocols in hand, we challenged our system in the reversible CO_2 hydrogenation/FA dehydrogenation process (Figure 4). **Ru-2** in EMIM OAc was chosen for the first set of experiments, in which each cycle was composed of an 18 (dark blue bars) or 72 (light blue bars) hydrogenation step, followed by a 4 h dehydrogenation step (dark red bars). As displayed in Figure 4a, the system was able to maintain its hydrogenation efficiency over 8 cycles, losing a significant part of it (lower than 50% FA/IL ratio) from the ninth cycle onward. On the other hand, the dehydrogenation process was kept close to completion over the whole study. Performing the same investigation with **Ru-1**, it was observed that a significant loss of hydrogenation efficiency was observed only after the 11th cycle (Figure 4b). The overall efficiency of the catalytic system, measured in terms of TON and gravimetric ratio of converted CO_2 over the mass of the reactor bed, proved to be high for both nitrosyl complexes tested in the hydrogenation/dehydrogenation cycles. The total TON was approximately 25,000 for both the systems (**Ru-1** achieved TON_{total} = 24,920 and **Ru-2** TON_{total} = 25,860); the gravimetric ratio was 1.95 employing **Ru-1** as a homogeneous catalyst and 2.17 for **Ru-2**. Moreover, compared to our previously reported system of ^{iPr}PNP-Ru(H)$_2$CO/EMIM OAc, which remains active for at least 13 cycles, both **Ru-1**/EMIM OAc and **Ru-2**/EMIM OAc seem less durable. We speculate whether the EMIM OAc coordinated complex PNP-Ru(EMIM)(OAc)-NO (vide infra) plays a role in this deactivation.

CONCLUSIONS

In summary, this work describes the use of PNP-Ru-NO and POP-Ru-NO complexes as catalysts for the reversible hydrogenation of CO_2 to formic acid using ionic liquids as solvents. Such protocols are the first examples of the use of nitrosyl complexes in the contexts of CO_2 capture and valorization and hydrogen storage and transportation.

Under the optimized conditions, the catalytic system was able to afford up to >95% yield of FA using EMIM OAc or BMIM OAc and could be subjected to several refilling steps reaching a maximum of 117% FA/IL. Importantly, we demonstrate that CO_2 can be first captured and then converted to FA in a sequence of two independent steps in one pot. The same system was also capable of promoting the dehydrogenation of FA at elevated temperatures, in which maximum conversion was achieved by using both EMIM OAc and BMIM OAc at 95 °C for 3 h. Hydrogenation/dehydrogenation cycles could be performed. The protocol described here offers, as the main advantage, more flexibility in terms of catalyst storage and manipulation, not requiring moisture avoidance and an inert atmosphere during both hydrogenation/dehydrogenation processes.

METHODS

Materials and Reagents

The ionic liquids (EMIM OAc (d = 1.101 g/mL used for calculations), BMIM OAc, EMIM $MeCO_3$, BMIM CO_2H, and EMIM $(EtO)_2PO_2$) were purchased from Iolitec and used without further purification. The complexes **Ru-1−Ru-6** were synthesized following the experimental procedures reported below. All catalyst syntheses were performed under inert conditions (Schlenk techniques or inert gas glovebox) unless otherwise stated. FA (98−100%) was purchased from Merck. Deuterated acetonitrile (CD_3CN) and deuterated dimethyl sulfoxide (DMSO-d_6) for NMR experiments were purchased from Merck. Deuterated dimethylformamide (DMF-d_7) was purchased from Eurisotop and deuterated methanol (CD_3OD) from Deutero. CO_2 gas ≥99,7% ($H_2O \leq 200$ ppm) was purchased from Airliquid. The H_2 gas ($H_2O \leq 3$ ppm; $O_2 \leq 2$ ppm) was purchased from Airliquid. NMR spectra were recorded on a Bruker Avance III 400 MHz spectrometer at room temperature. Chemical shifts are expressed in ppm relative to tetramethylsilane and are referenced against the solvent peak.[58]

The reactor employed 2550 flat gasket micro vessel, Alloy 600, reactor capacity: 20 mL; PTFE cup volume: 6.0 mL. The pressure gauge is nonelectronic and subject to error.

Instrumentations

All crystals were submerged in polybutene oil (Sigma, >90%) as protection against oxidation and hydrolysis by air. Suitable crystals

https://doi.org/10.1021/jacsau.5c00051
JACS Au 2025, 5, 2114−2122

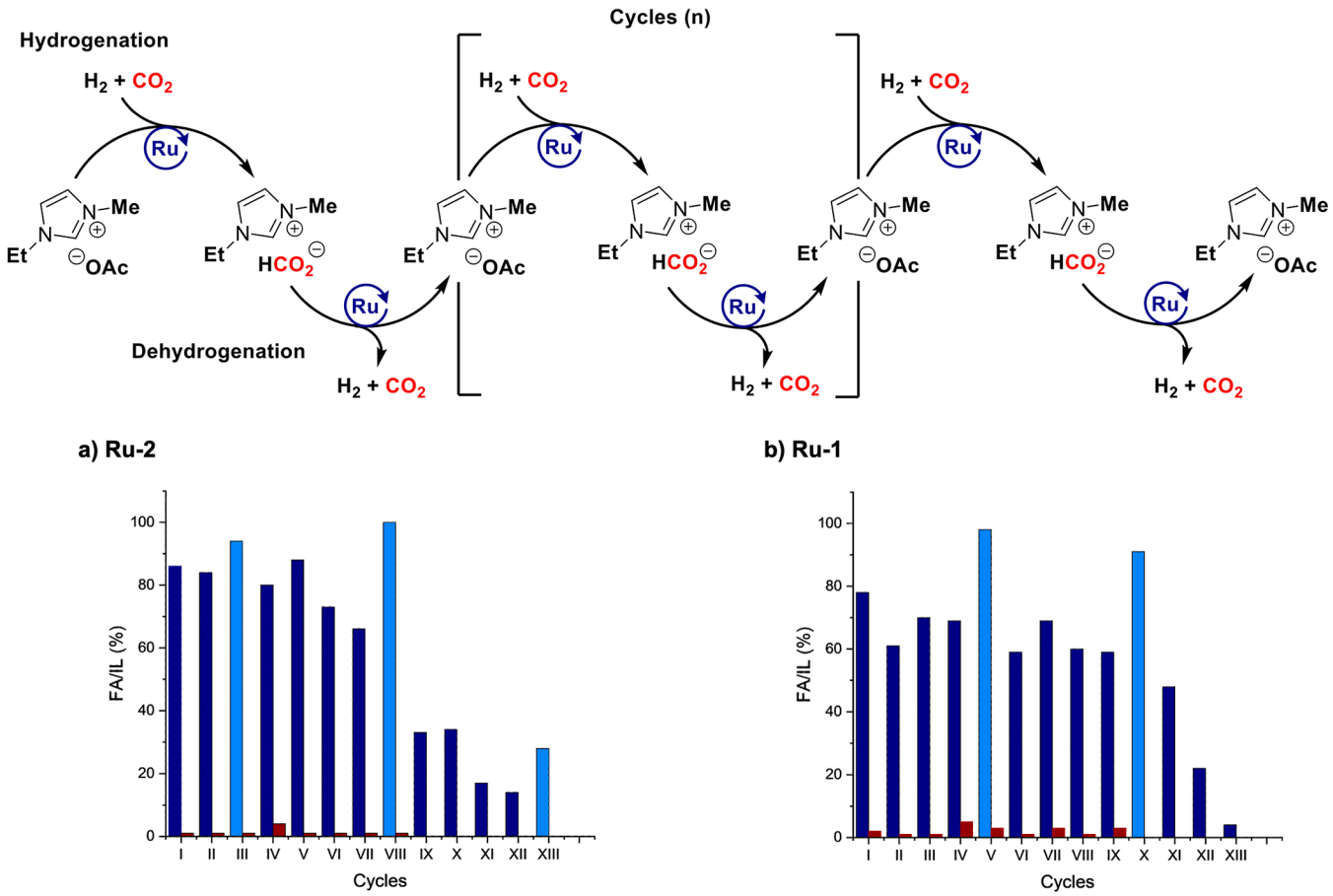

Figure 4. Reversible CO_2 hydrogenation/FA dehydrogenation studies: (a) CO_2 hydrogenation/FA dehydrogenation cycles performed with **Ru-2** and (b) CO_2 hydrogenation/FA dehydrogenation cycles performed with **Ru-1**. General conditions: Hydrogenation (dark blue bars = 18 h, light blue bars = 72 h): **Ru-1** (0.004 mmol, 0.05 mol %), EMIM OAc (1 mL), CO_2/H_2 (10:20 bar), 30 °C; dehydrogenation (red bars): **Ru-2** (0.004 mmol), EMIM OAc (1 mL), 4 h, 95 °C.

were identified using light microscopy and harvested with a MiTeGen cryo loop. They were mounted on a 5-axis goniometer attached to a Rigaku SuperNova dual source CCD-diffractometer. The measurements were conducted at 120 K using either Mo or Cu Kα radiation. Structures were solved using Olex2[59] equipped with SHELXT[3] software using intrinsic phasing and refined to completion using SHELXL[60] employing least-squares minimizations against F^2. Structure factors regarding the solvent molecules were filtered out in cases of a high disorder using Platon squeeze.[61] In all depictions, cocrystallized solvents and hydrogen atoms on carbon are omitted for clarity. Thermal ellipsoids are plotted at the 50% probability level. All depictions follow the same color code: hydrogen white, boron bright yellow, carbon gray, nitrogen light blue, oxygen red, fluorine bright green, sulfur yellow, phosphorus purple, chlorine dark green, and ruthenium dark blue.

Attenuated total reflectance infrared spectroscopy (ATR-IR) was performed on a Bruker Optics VERTEX 80 vacuum Fourier-transform spectrometer equipped with a germanium on a KBr beam splitter and a LN_2-cooled HgCdTe detector. A global radiation source was used. The solid samples were pressed against a single-reflection germanium crystal or a diamond ATR surface. Signals of water vapor and baseline drift were corrected by subtraction of a blank run and ATR corrections were applied to compensate for wavelength-dependent penetration depth.

HRMS measurements were taken on a Thermo Fisher Orbitrap Exploris 120, mounted with an H-ESI source. All spectra were recorded at 30,000 fwhm resolution. For analysis of the FADH reaction mixtures: an aliquot was collected (at the first 45 min and after 2 cycles and 3 h, respectively) and dissolved in MeOH/MiliQ water (50:50 v/v) under a N_2 atmosphere, passed through a syringe filter and injected into the HRMS spectrometer.

GC-TCD measurements were taken on an Agilent Technologies 6890 M Network GC system.

EXPERIMENTAL PROCEDURES

Synthesis of Ru-1

As previously reported,[55] inside the glovebox, a 10 mL vial equipped with a stirring bar was charged with a 10% solution of bis(2-diisopropylphosphinoethyl)amine in THF (251 mg, 0.822 mmol, 1.05 equiv) and an additional amount of THF (approximately 5 mL). To this solution, $Ru(NO)Cl_3{\cdot}H_2O$ (200 mg, 0.783 mmol, 1.0 equiv) was added in one portion, and the resulting dark violet suspension was stirred overnight, turning into a pinkish suspension. The pink powdery product was filtered off under ambient conditions, washed with acetonitrile until a colorless filtrate appeared, followed by washing with Et_2O, and dried in air. High-quality single crystals were obtained by the vapor diffusion of Et_2O into a concentrated ethanolic solution of the compound at room temperature. Yield: 87% (370 mg, 0.682 mmol).

Synthesis of Ru-2–Ru-5

As previously reported,[55] under ambient conditions, **Ru-1** (200 mg, 0.37 mmol, 1.0 equiv) was transferred to a 10 mL vial and dissolved in 3 mL of water. To the resulting red solution was added a solution of NaX (X = BF_4^-, BPh_4^-, PF_6^-, OTs^-) (0.37 mmol, 1.0 equiv) in 5 mL of H_2O dropwise under vigorous stirring because a pinkish precipitate starts to be formed immediately after the first drops of the solution are added. The flask was closed and stirred at rt overnight. Afterward, the

https://doi.org/10.1021/jacsau.5c00051
JACS Au 2025, 5, 2114–2122

pinkish precipitate was filtered off on a glass filter funnel or through a glass filter paper and washed several times with water. The product was extracted with acetonitrile (3−5 mL) and the residual NaCl was filtered off through a glass filter paper. The solvent was removed in vacuo to afford the respective product.

Synthesis of Ru-6

In a 20 mL vial equipped with a stir bar, $Ru(NO)Cl_3{\cdot}H_2O$ (175 mg,0.77 mmol, 1.0 equiv) and (9,9-dimethyl-9*H*-xanthene-4,5-diyl)-bis(diphenylphosphane) ("xantphos") (493 mg, 0.85 mmol, 1.1 equiv) were dissolved in benzene (15 mL). The solution was stirred at room temperature for 96 h, during which a beige solid precipitated. The solvent was removed, the product was washed three times in 5 mL hexane, dried in vacuo, and was obtained as a beige powder (522 mg, 0.54 mmol, 83%). Crystals of sufficient quality for SC-XRD can be obtained by dissolving in DMSO in high concentrations and layering with diethyl ether in a 20 mL vial at room temperature.

General Procedure for the Hydrogenation of CO_2

The high-pressure reactor was loaded with a stir bar, ionic liquid, and catalyst. The reactor was flushed with CO_2 three times to remove air before applying the desired pressure of CO_2/H_2 and the specific temperature for 18 h under stirring (420 rpm). The reaction was cooled with an ice-bath (when above room temperature), the remaining pressure carefully released, and the reaction mixture was analyzed by ^{1}H NMR using the ionic liquid as an internal reference. For the refilling experiments, the same pressure of the CO_2/H_2 mixture was applied in every repetition after flushing the reactor three times with CO_2.

General Procedure for the Dehydrogenation of Formic Acid

A two-neck flask containing a magnetic stir bar and equipped with an air-cooled condenser was charged with the catalyst. The set up was connected to a Schlenk line; the atmosphere was exchanged to argon, and the ionic liquid (1.0 mL) was added. The mixture was stirred at the chosen temperature until a complete solution of the catalyst was obtained. Formic acid was added with a gentle flow of argon to facilitate the hydrogen release. For the initial screening, an aliquot was taken by a syringe for ^{1}H NMR analysis at different time intervals (15 min, 30 min, 45 min, 1 h, 1.5 h, 2 h, 2.5 h, 3 h), totaling 3 h. After this period, the reaction mixture was cooled to room temperature and analyzed again by ^{1}H NMR.

General Procedure for the Hydrogenation/Dehydrogenation Cycle Experiments

The first hydrogenation step was performed as described in the general procedure for CO_2 hydrogenation. After 18 h, the gas was carefully released, the reactor was opened, and a sample for ^{1}H NMR analysis was taken. Afterward, the reactor was closed, but the gas outlet was kept open to allow the release of CO_2. The system was warmed up to 95 °C and kept at this temperature for 4 h for the dehydrogenation step. Similarly, after the dehydrogenation process, the pressure reactor was cooled to room temperature and opened to take a sample for NMR analysis. This procedure was repeated several times until catalytic activity was completely lost.

■ ASSOCIATED CONTENT

Supporting Information

The Supporting Information is available free of charge at https://pubs.acs.org/doi/10.1021/jacsau.5c00051.

Synthetic procedures, NMRs, IRs, EAs, HRMS, and crystallographic data (PDF)

■ AUTHOR INFORMATION

Corresponding Author

Martin Nielsen − *Department of Chemistry, Technical University of Denmark, 2800 Kgs. Lyngby, Denmark;* orcid.org/0000-0002-3170-1198; Email: marnie@kemi.dtu.dk

Authors

José Tiago M. Correia − *Department of Chemistry, Technical University of Denmark, 2800 Kgs. Lyngby, Denmark; Department of Fundamental Chemistry, Chemistry Institute, University of São Paulo, 05508-000 São Paulo, Brazil*

Valeria Nori − *Department of Chemistry, Technical University of Denmark, 2800 Kgs. Lyngby, Denmark*

Mike S. B. Jørgensen − *Department of Chemistry, Technical University of Denmark, 2800 Kgs. Lyngby, Denmark;* orcid.org/0000-0002-6968-1225

Alexander T. Nikol − *Department of Chemistry, Technical University of Denmark, 2800 Kgs. Lyngby, Denmark*

Complete contact information is available at: https://pubs.acs.org/10.1021/jacsau.5c00051

Author Contributions

†J.T.M.C. and V.N. authors contributed equally. MN and JTMC conceptualized the project. MN, JTMC, and VN conceived and designed the project. MSBJ and ATN developed the complex salts. JTMC and VN carried out the catalysis optimization. JTMC, VN, MSBJ, and ATN carried out the data curation. JT and VN wrote the original manuscript. All authors revised the manuscript. MN did project administration and funding acquisition. All authors have given approval to the final version of the manuscript. CRediT: **José Tiago Menezes Correia** conceptualization, data curation, formal analysis, investigation, methodology, visualization, writing - original draft, writing - review & editing; **Valeria Nori** data curation, formal analysis, investigation, methodology, validation, visualization, writing - original draft, writing - review & editing; **Mike S. B. Jørgensen** data curation, formal analysis, investigation, methodology, validation, writing - review & editing; **Alexander Nikol** data curation, formal analysis, investigation, validation, writing - review & editing; **Martin Nielsen** conceptualization, funding acquisition, methodology, project administration, resources, supervision, writing - review & editing.

Funding

The authors are grateful to the VILLUM FONDEN (19049 and 53069), Carlsberg Foundation (CF20-0365), Independent Research Fund Denmark (1127-00172B), Novo Nordisk Foundation (NNF20OC0064560), and COWI Foundation (A-149.10).

Notes

The authors declare no competing financial interest.

■ ACKNOWLEDGMENTS

We thank Mikroanalytisches Laboratorium Kolbe for carrying out Elemental Analysis and René Wugt Larsen for carrying out IR analysis.

■ REFERENCES

(1) *Green Carbon Dioxide: Advances in CO_2 Utilization*, 1st ed.; Centi, G., Perathoner, S., Eds.; John Wiley & Sons, 2014.

(2) Cuéllar-Franca, R. M.; Azapagic, A. Carbon Capture, Storage and Utilisation Technologies: A Critical Analysis and Comparison of Their Life Cycle Environmental Impacts. *J. CO_2 Util.* **2015**, *9*, 82−102.

(3) Sancho-Sanz, I.; Korili, S. A.; Gil, A. Catalytic valorization of CO_2 by hydrogenation: current status and future trends. *Catal. Rev.* **2023**, *65* (3), 698−772.
(4) Modak, A.; Bhanja, P.; Dutta, S.; Chowdhury, B.; Bhaumik, A. Catalytic reduction of CO_2 into fuels and fine chemicals. *Green Chem.* **2020**, *22*, 4002−4033.
(5) Dibenedetto, A.; Angelini, A.; Stufano, P. Use of carbon dioxide as feedstock for chemicals and fuels: homogeneous and heterogeneous catalysis. *J. Chem. Technol. Biotechnol.* **2014**, *89*, 334−353.
(6) Müller, K.; Brooks, K.; Autrey, T. Hydrogen Storage in Formic Acid: A Comparison of Process Options. *Energy Fuels* **2017**, *31* (11), 12603−12611.
(7) Guo, J.; Yin, C. K.; Zhong, D. L.; Wang, Y. L.; Qi, T.; Liu, G. H.; Shen, L. T.; Zhou, Q. S.; Peng, Z. H.; Yao, H.; Li, X. B. Formic Acid as a Potential On-Board Hydrogen Storage Method: Development of Homogeneous Noble Metal Catalysts for Dehydrogenation Reactions. *ChemSusChem* **2021**, *14* (13), 2655−2681.
(8) Sordakis, K.; Tang, C.; Vogt, L. K.; Junge, H.; Dyson, P. J.; Beller, M.; Laurenczy, G. Homogeneous Catalysis for Sustainable Hydrogen Storage in Formic Acid and Alcohol. *Chem. Rev.* **2018**, *118* (2), 372−433.
(9) Mellmann, D.; Sponholz, P.; Junge, H.; Beller, M. Formic acid as a hydrogen storage material − development of homogeneous catalysts for selective hydrogen release. *Chem. Soc. Rev.* **2016**, *45*, 3954−3988.
(10) Loges, B.; Boddien, A.; Gärtner, F.; Junge, H.; Beller, M. Catalytic Generation of Hydrogen from Formic acid and its Derivatives: Useful Hydrogen Storage Materials. *Top. Catal.* **2010**, *53*, 902−914.
(11) Ma, Z.; Legrand, U.; Pahija, E.; Tavares, J. R.; Boffito, D. C. From CO_2 to Formic Acid Fuel Cells. *Ind. Eng. Chem. Res.* **2021**, *60* (2), 803−815.
(12) van Putten, R.; Wissink, T.; Swinkels, T.; Pidko, E. A. Fuelling the hydrogen economy: Scale-up of an integrated formic acid-to-power system. *Int. J. Hydrogen Energy* **2019**, *44* (53), 28533−28541.
(13) Hsu, S. F.; Rommel, S.; Eversfield, P.; Muller, K.; Klemm, E.; Thiel, W. R.; Plietker, B. A Rechargeable Hydrogen Battery Based on Ru Catalysis. *Angew. Chem., Int. Ed.* **2014**, *53*, 7074−7078.
(14) Filonenko, G. A.; van Putten, R.; Schulpen, E. N.; Hensen, E. J. M.; Pidko, E. A. Highly Efficient Reversible Hydrogenation of Carbon Dioxide to Formates Using a Ruthenium PNP-Pincer Catalyst. *ChemCatChem* **2014**, *6* (6), 1526−1530.
(15) Kothandaraman, J.; Czaun, M.; Goeppert, A.; Haiges, R.; Jones, J. P.; May, R. B.; Prakash, G. K. S.; Olah, G. A. Amine-Free Reversible Hydrogen Storage in Formate Salts Catalyzed by Ruthenium Pincer Complex without pH Control or Solvent Change. *ChemSusChem* **2015**, *8* (8), 1442−1451.
(16) Verron, R.; Puig, E.; Sutra, P.; Igau, A.; Fischmeister, C. Base-Free Reversible Hydrogen Storage Using a Tethered π-Coordinated-Phenoxy Ruthenium-Dimer Precatalyst. *ACS Catal.* **2023**, *13* (9), 5787−5794.
(17) Wei, D.; Sang, R.; Sponholz, P.; Junge, H.; Beller, M. Reversible Hydrogenation of Carbon Dioxide to Formic Acid Using a Mn-Pincer Complex in the Presence of Lysine. *Nat. Energy* **2022**, *7* (5), 438−447.
(18) Kushwaha, S.; Parthiban, J.; Singh, S. K. Recent Developments in Reversible CO_2 Hydrogenation and Formic Acid Dehydrogenation over Molecular Catalysts. *ACS Omega* **2023**, *8* (42), 38773−38793.
(19) Piccirilli, L.; Rabell, B.; Padilla, R.; Riisager, A.; Das, S.; Nielsen, M. Versatile CO_2 Hydrogenation-Dehydrogenation Catalysis with a Ru-PNP/Ionic Liquid System. *J. Am. Chem. Soc.* **2023**, *145* (10), 5655−5663.
(20) Nikol, A. T.; Rabell, B.; Jørgensen, M. S. B.; Larsen, R. W.; Nielsen, M. Formic acid dehydrogenation using Ruthenium-POP pincer complexes in ionic liquids. *Sci. Rep.* **2024**, *14*, 26209.
(21) Aufricht, P.; Nori, V.; Rabell, B.; Piccirilli, L.; Koranchalil, S.; W Larsen, R.; Nielsen, M.; Nielsen, M. Formic acid dehydrogenation catalysed by a novel amino-di(N-heterocyclic carbene) based Ru-CNC pincer complex. *Chem. Commun.* **2025**, *61*, 3986−3989.
(22) *Nitrosyl Complexes in Inorganic Chemistry, Biochemistry and Medicine I*; Mingos, D. M. P., Ed.; Springer Verlag: Berlin Heidelberg, 2014.
(23) *Nitrosyl Complexes in Inorganic Chemistry, Biochemistry and Medicine II*; Mingos, D. M. P., Ed.; Springer Verlag: Berlin Heidelberg, 2014.
(24) Tfouni, E.; Truzzi, D. R.; Tavares, A.; Gomes, A. J.; Figueiredo, L. E.; Franco, D. W. Biological Activity of Ruthenium Nitrosyl Complexes. *Nitric Oxide—Biol. Chem.* **2012**, *26* (1), 38−53.
(25) Negri, L. B.; Martins, T. J.; Ramos, L. C. B.; da Silva, R. S. Nitric Oxide Derivative Ruthenium Compounds as NO-Based Chemotherapeutic and Phototherapeutic Agents. In *Nitric Oxide Donors*; Seabra, A. B., Ed.; Academic Press, 2017; pp 1−24..
(26) Stepanenko, I.; Zalibera, M.; Schaniel, D.; Telser, J.; Arion, V. B. Ruthenium-Nitrosyl Complexes as NO-Releasing Molecules, Potential Anticancer Drugs, and Photoswitches Based on Linkage Isomerism. *Dalt. Trans.* **2022**, *51* (14), 5367−5393.
(27) Dybov, A.; Blacque, O.; Berke, H. Molybdenum Nitrosyl Complexes and Their Application in Catalytic Imine Hydrogenation Reactions. *Eur. J. Inorg. Chem.* **2011**, *2011* (5), 652−659.
(28) Dudle, B.; Rajesh, K.; Blacque, O.; Berke, H. Rhenium in Homogeneous Catalysis: [ReBrH(NO)(Labile Ligand)(Large-Bite-Angle Diphosphine)] Complexes as Highly Active Catalysts in Olefin Hydrogenations. *J. Am. Chem. Soc.* **2011**, *133* (21), 8168−8178.
(29) Chakraborty, S.; Blacque, O.; Fox, T.; Berke, H. Trisphosphine-Chelate-Substituted Molybdenum and Tungsten Nitrosyl Hydrides as Highly Active Catalysts for Olefin Hydrogenations. *Chem.—Eur. J.* **2014**, *20* (39), 12641−12654.
(30) Jiang, Y.; Berke, H. Dehydrocoupling of Dimethylamine-Borane Catalysed by Rhenium Complexes and Its Application in Olefin Transfer-Hydrogenations. *Chem. Commun.* **2007**, *34*, 3571−3573.
(31) Landwehr, A.; Dudle, B.; Fox, T.; Blacque, O.; Berke, H. Bifunctional Rhenium Complexes for the Catalytic Transfer-Hydrogenation Reactions of Ketones and Imines. *Chem.—Eur. J.* **2012**, *18* (18), 5701−5714.
(32) Choualeb, A.; Maccaroni, E.; Blacque, O.; Schmalle, H. W.; Berke, H. Rhenium Nitrosyl Complexes for Hydrogenations and Hydrosilylations. *Organometallics* **2008**, *27* (14), 3474−3481.
(33) Jiang, Y.; Blacque, O.; Fox, T.; Frech, C.; Berke, H. Highly Selective Dehydrogenative Silylation of Alkenes Catalyzed by Rhenium Complexes. *Chem.—Eur. J.* **2009**, *15* (9), 2121−2128.
(34) Dong, H.; Berke, H. A Convenient and Efficient Rhenium-Catalyzed Hydrosilylation of Ketones and Aldehydes. *Adv. Synth. Catal.* **2009**, *351* (11−12), 1783−1788.
(35) Kathó, A.; Opre, Z.; Laurenczy, G.; Joó, F. Water-soluble analogs of $[RuCl_3(NO)(PPh_3)_2]$ and their catalytic activity in the hydrogenation of carbon dioxide and bicarbonate in aqueous solution. *J. Mol. Catal. A: Chem.* **2003**, *204−205*, 143−148.
(36) Plietker, B.; Dieskau, A. The Reincarnation of the Hieber Anion $[Fe(CO)_3(NO)]$-a New Venue in Nucleophilic Metal Catalysis. *Eur. J. Org Chem.* **2009**, *2009* (6), 775−787.
(37) Zhang, D. H.; Knelles, J.; Plietker, B. Iron-Catalyzed Michael Addition of Ketones to Polar Olefins. *Adv. Synth. Catal.* **2016**, *358* (15), 2469−2479.
(38) Kramm, F.; Teske, J.; Ullwer, F.; Frey, W.; Plietker, B. Annelated Cyclobutanes by Fe-Catalyzed Cycloisomerization of Enyne Acetates. *Angew. Chem., Int. Ed.* **2018**, *57* (40), 13335−13338.
(39) Baykal, A.; Plietker, B. A. $Bu_4N[Fe(CO)_3(NO)]$-Catalyzed Hemetsberger−Knittel Indole Synthesis. *Eur. J. Org Chem.* **2020**, *2020* (9), 1145−1147.
(40) Choualeb, A.; Lough, A. J.; Gusev, D. G. Hydridic Rhenium Nitrosyl Complexes with Pincer-Type PNP Ligands. *Organometallics* **2007**, *26* (14), 3509−3515.
(41) Fogler, E.; Iron, M. A.; Zhang, J.; Ben-David, Y.; Diskin-Posner, Y.; Leitus, G.; Shimon, L. J. W.; Milstein, D. Ru(0) and Ru(II) Nitrosyl Pincer Complexes: Structure, Reactivity, and Catalytic Activity. *Inorg. Chem.* **2013**, *52* (19), 11469−11479.
(42) Pecak, J.; Stöger, B.; Mastalir, M.; Veiros, L. F.; Ferreira, L. P.; Pignitter, M.; Linert, W.; Kirchner, K. Five-Coordinate Low-Spin

{FeNO} 7 PNP Pincer Complexes. *Inorg. Chem.* **2019**, *58* (7), 4641−4646.
(43) Pecak, J.; Eder, W.; Stöger, B.; Realista, S.; Martinho, P. N.; Calhorda, M. J.; Linert, W.; Kirchner, K. Synthesis, Characterization, and Catalytic Reactivity of {CoNO}8 PCP Pincer Complexes. *Organometallics* **2020**, *39* (14), 2594−2601.
(44) Pecak, J.; Fleissner, S.; Veiros, L. F.; Pittenauer, E.; Stöger, B.; Kirchner, K. Synthesis and Catalytic Reactivity of Cobalt Pincer Nitrosyl Hydride Complexes. *Organometallics* **2021**, *40* (2), 278−285.
(45) Zhang, J.; Leitus, G.; Ben-David, Y.; Milstein, D. Efficient Homogeneous Catalytic Hydrogenation of Esters to Alcohols. *Angew. Chem., Int. Ed.* **2006**, *45*, 1113−1115.
(46) Kuriyama, W.; Matsumoto, T.; Ogata, O.; Ino, Y.; Aoki, K.; Tanaka, S.; Ishida, K.; Kobayashi, T.; Sayo, N.; Saito, T. Catalytic Hydrogenation of Esters. Development of an Efficient Catalyst and Processes for Synthesising (R)-1,2-Propanediol and 2-(l-Menthoxy)-Ethanol. *Org. Process Res. Dev.* **2012**, *16* (1), 166−171.
(47) Rezayee, N. M.; Huff, C. A.; Sanford, M. S. Tandem Amine and Ruthenium-Catalyzed Hydrogenation of CO_2 to Methanol. *J. Am. Chem. Soc.* **2015**, *137* (3), 1028−1031.
(48) Farrar-Tobar, R. A.; Wei, Z.; Jiao, H.; Hinze, S.; de Vries, J. G. Selective Base-Free Transfer Hydrogenation of α,β-Unsaturated Carbonyl Compounds Using *i*PrOH or EtOH as Hydrogen Source. *Chem.—Eur. J.* **2018**, *24* (11), 2725−2734.
(49) Padilla, R.; Jørgensen, M. S. B.; Paixão, M. W.; Nielsen, M. Efficient Catalytic Hydrogenation of Alkyl Levulinates to γ-Valerolactone. *Green Chem.* **2019**, *21* (19), 5195−5200.
(50) Padilla, R.; Koranchalil, S.; Nielsen, M. Efficient and Selective Catalytic Hydrogenation of Furanic Aldehydes Using Well Defined Ru and Ir Pincer Complexes. *Green Chem.* **2020**, *22* (20), 6767−6772.
(51) Pinheiro, D. L. J.; Nielsen, M. Base-Free Synthesis of Furfurylamines from Biomass Furans Using Ru Pincer Complexes. *Catalysts* **2021**, *11* (5), 558−568.
(52) Pinheiro, D. L. J.; Nielsen, M. Chemoselective Transfer Hydrogenation of Enamides Using Ru Pincer Complexes for the Synthesis of α-Amino Acids. *J. Org. Chem.* **2022**, *87* (8), 5419−5423.
(53) Ni, Z.; Padilla, R.; dos Santos Mello, L.; Nielsen, M. Tuning Ethanol Upgrading toward Primary or Secondary Alcohols by Homogeneous Catalysis. *ACS Catal.* **2023**, *13* (8), 5449−5455.
(54) Koranchalil, S. M.; Nielsen, M. Direct biomass valorisation to γ-valerolactone by Ru-PNP catalysed hydrogenation in acid. *EES. Catal.* **2024**, *2*, 803−810.
(55) Correia, M. J. T.; Pinheiro, L. J. D.; Jørgensen, M. S. B.; Larsen, R. W.; Nielsen, M. Ruthenium Pincer Nitrosyl Complex Salts in Catalytic Transfer Hydrogenations under Mild Conditions. *ChemCatChem* **2025**, No. e20240197417.
(56) Shukla, S. K.; Khokarale, S. G.; Bui, T. Q.; Mikkola, J.-P. T. Ionic Liquids: Potential Materials for Carbon Dioxide Capture and Utilization. *Front. Mater.* **2019**, *6*, 42.
(57) Qadir, M. I.; Castegnaro, M. V.; Selau, F. F.; Baptista, D. L.; Chacon, G.; Pontes, R. B.; Lisbôa, A. M.; Eberhardt, D.; Dupont, J. Dynamic tuning of naked ruthenium clusters/nanoparticles in ionic liquids cages to boost CO2 hydrogenation to formic acid. *Applied Catalysis B: Environmental* **2024**, *341*, 123315.
(58) Fulmer, G. R.; Miller, A. J. M.; Sherden, N. H.; Gottlieb, H. E.; Nudelman, A.; Stoltz, B. M.; Bercaw, J. E.; Goldberg, K. I. NMR Chemical Shifts of Trace Impurities: Common Laboratory Solvents, Organics, and Gases in Deuterated Solvents Relevant to the Organometallic Chemist. *Organometallics* **2010**, *29*, 2176−2179.
(59) Dolomanov, O. V.; Bourhis, L. J.; Gildea, R. J.; Howard, J. A. K.; Puschmann, H. OLEX2: a complete structure solution, refinement and analysis program. *J. Appl. Crystallogr.* **2009**, *42*, 339−341.
(60) Sheldrick, G. M. SHELXT − Integrated space-group and crystalstructure determination. *Acta Crystallogr.* **2015**, *A71*, 3−8.
(61) Spek, L. A. PLATON SQUEEZE: a tool for the calculation of the disordered solvent contribution to the calculated structure factors. *Acta Crystallogr.* **2015**, *C71*, 9−18.

https://doi.org/10.1021/jacsau.5c00051
JACS Au 2025, 5, 2114−2122